



DEEPEYES: INCENTIVIZING “THINKING WITH IMAGES” VIA REINFORCEMENT LEARNING

Ziwei Zheng^{1,2*}, Michael Yang^{1*}, Jack Hong^{1*}, Chenxiao Zhao^{1*†},
Guohai Xu^{1‡}, Le Yang^{2‡}, Chao Shen², Xing Yu¹

¹Xiaohongshu Inc., ²Xi’an Jiaotong University

* Equal contribution, Random order † Main Code Contributor ‡ Corresponding Author

Project Homepage

{chenxiao2, xuguohai}@xiaohongshu.com, yangle15@xjtu.edu.cn,
ziwei.zheng@stu.xjtu.edu.cn, {yangminghao199, jaaackhong}@gmail.com

ABSTRACT

Large Vision-Language Models excel at multimodal understanding but struggle to deeply integrate visual information into their predominantly text-based reasoning processes, a key challenge in mirroring human cognition. To address this, we introduce *DeepEyes*, a model that learns to “think with images”, trained end-to-end with reinforcement learning without requiring pre-collected reasoning data for cold-start supervised fine-tuning (SFT). Notably, this ability emerges natively, leveraging the model’s own grounding capability as an intrinsic function rather than relying on external specialized models or APIs. We enable this capability through active perception, where the model learns to strategically ground its reasoning in visual information, guided by a tailored data selection and reward strategy. *DeepEyes* achieves significant performance gains on general perception and reasoning benchmarks and also demonstrates improvement in grounding, hallucination, and mathematical reasoning tasks. Interestingly, we observe the distinct evolution of active perception from initial exploration to efficient and accurate exploitation, and diverse thinking patterns that closely mirror human visual reasoning processes. Code is available at <https://github.com/Visual-Agent/DeepEyes>.

1 INTRODUCTION

Recent advances in Vision-Language Models (VLMs) have enabled deeper reasoning over multimodal inputs by adopting long Chain-of-Thought (CoT) approaches (Team et al., 2025a;b; Guo et al., 2025b), allowing these models to handle more complex tasks. However, these models still primarily rely on text-based reasoning, with their thought processes largely confined to the language modality. In contrast, human reasoning naturally combines vision and cognition, thinking with images by extracting information through sequential visual fixations, which support more accurate perceptual decision-making, which was essential for survival in early human evolution (Najemnik & Geisler, 2005). While some recent works have proposed pre-defined workflow-based strategies to incorporate visual information into CoT reasoning (Shao et al., 2024a; Sun et al., 2024), the modular designs suffer from suboptimal performance (Ross et al., 2011).

In a recent milestone, the OpenAI o3 model (OpenAI, 2025) has successfully integrated visual information as a dynamic element in the reasoning process. The o3 transcends the language-modality confinement by extending reasoning capability to “thinking with images” like humans. Additionally, it resolves the coordination limitations by combining textual CoT and image manipulation tools in a naturally interleaved fashion during the CoT process. This approach enables a new axis for test-time

*Work done during Ziwei’s internship at Xiaohongshu. The specific contribution of co-first authors is shown in the Appendix.C.

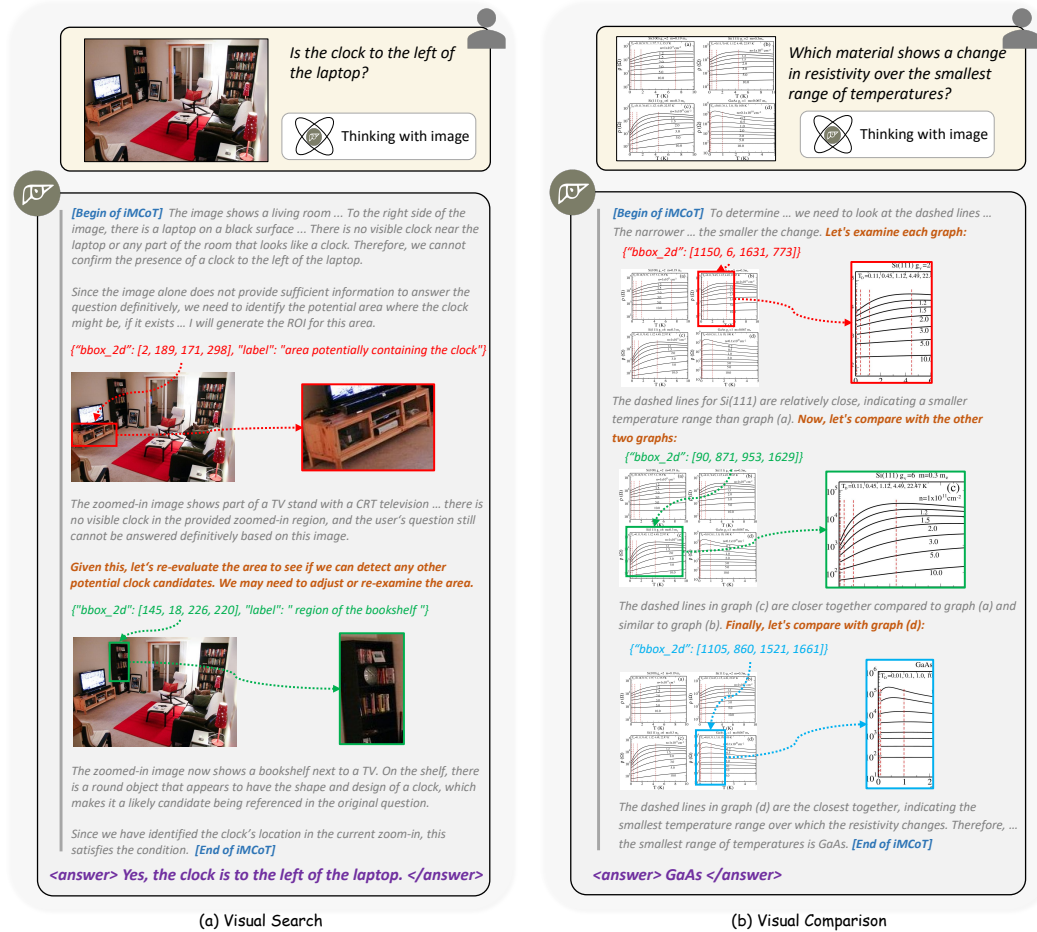


Figure 1: **Interleaved Multi-modal Chain-of-Thought (iMCoT)**. *DeepEyes* is incentivized to perform active perception throughout the reasoning process with end-to-end reinforcement learning.

compute scaling by seamlessly integrating visual and textual reasoning, representing a meaningful advancement toward true multimodal reasoning. However, the inner mechanism remains undisclosed to the open-source community.

In this paper, we introduce *DeepEyes*, a model with “thinking with images” ability, which is incentivized via end-to-end reinforcement learning. This capability emerges natively without relying on separate specialized models and is directly guided by outcome rewards, eliminating the need for cold-start supervised fine-tuning used in previous methods. Specifically, we encapsulate the model’s grounding ability in an active perception mechanism, enabling it to gather information from the original image within an agentic framework. As shown in Figure 1, the model adaptively generates image grounding coordinates and crops relevant regions, which are then incorporated into the ongoing reasoning trajectory. This supports an interleaved Multimodal Chain-of-Thought (iMCoT), where visual and textual reasoning are seamlessly integrated.

In early attempts, we observe that the model struggles to effectively utilize its active perception capability. Specifically, it is reluctant to perform image zoom-ins and even when it does, the exploration often selects suboptimal regions. This results in low rewards and unstable training dynamics. To address these issues, we propose a data selection mechanism to choose training samples based on their potential to encourage active perception behavior. Additionally, we design a reward strategy that assigns a conditional bonus to the trajectories that successfully complete their tasks through active perception. Our ablation studies validate that these two strategies are crucial for optimizing the efficiency and accuracy of active perception.

Without supervised fine-tuning (SFT) for intermediate reasoning steps, we observe the model’s active perception strategy evolving through three distinct stages during RL training: (1) initial, ineffective

exploration; followed by (2) frequent and effective application of the capability; and finally, (3) a mature, selective, and efficient approach yielding high performance. This progression demonstrates the model’s growing mastery of its visual reasoning capabilities through active perception. Additionally, diverse iMCoT reasoning patterns emerge, such as visual search for small or hard-to-recognize objects, visual comparisons across different regions, visual confirmation to eliminate uncertainty, and hallucination mitigation by focusing on details. These diverse reasoning behaviors closely resemble human cognitive processes, thereby enhancing the system’s overall multimodal capabilities.

Experimental results show that *DeepEyes* can significantly boost performance on multiple visual perception and reasoning tasks. For high-resolution benchmarks, *DeepEyes* with a 7B model achieves an accuracy of 90.1% (+18.9 %) on V^* , and improves HR-Bench-4K and HR-Bench-8K by 6.3% and 7.3%, respectively. In addition, *DeepEyes* also improves multimodal capabilities on a wide range of tasks such as visual grounding, hallucination mitigation, and mathematical problem solving. The main contributions are summarized as follows:

- We incentivize and enhance the ability of thinking with images via end-to-end reinforcement learning, forming iMCoT that seamlessly blends visual-textual reasoning without requiring cold-start SFT or separate specialized models as external tools.
- To better incentivize the model’s interleaving reasoning, we introduce an active-perception data selection mechanism and a tailored reward strategy that promote grounding-assisted problem solving. Experiments show that both components significantly advance iMCoT.
- We reveal the intriguing RL training dynamic of iMCoT, where active perception behavior undergoes distinct stages, evolving from initial exploration to efficient and accurate exploitation. We also observe diverse reasoning patterns, such as visual search, comparison, and confirmation.

2 RELATED WORK

Multi-modal Large Language Models. Multimodal large language models (MLLMs) have evolved from early systems that loosely combined vision encoders with language models into more integrated architectures through joint training. Methods such as BLIP-2 (Li et al., 2023b) and LLaVA (Liu et al., 2023b;a) align visual and linguistic modalities by projecting image features into the latent space of frozen LLMs using query transformers or lightweight projectors, enabling tasks like visual question answering and instruction following. To address resolution constraints, approaches like AnyRes (Liu et al., 2024a; Chen et al., 2024a) allow for flexible image sizes and enhanced visual fidelity. These advances have led to strong open-source models, including the LLaVA (Liu et al., 2024b; Guo et al., 2024; Zhang et al., 2025b; Lin et al., 2023; Li et al., 2023a), Qwen-VL (Bai et al., 2023; Wang et al., 2024b; Yang et al., 2024), and InternVL (Chen et al., 2024c; Gao et al., 2024; Lu et al., 2025) series. Concurrently, large-scale models like Flamingo (Alayrac et al., 2022), mPLUG-Owl (Ye et al., 2023; 2024b;a), and GPT-4V (Yang et al., 2023) aim to unify vision-language understanding, incorporating mechanisms such as mixture-of-experts (Shu et al., 2024; Li et al., 2025c; Shen et al., 2024b) or image generation (Xie et al., 2024; Xu et al., 2025). However, these models lack reasoning capabilities like Chain-of-Thought and test-time scalability (Muennighoff et al., 2025; Zhang et al., 2025a; Chen et al., 2024b), and still decouple perception from reasoning.

Vision-language Model Reasoning. Existing Multimodal Chain-of-Thought (MCoT) reasoning methods fall into two main categories. Early approaches rely on predefined workflows or auxiliary models (Liu et al., 2024c; Mondal et al., 2024; Luo et al., 2024), often focusing on region-of-interest localization (Wu & Xie, 2024; Fu et al., 2025; Wei et al., 2025; Li et al., 2025b), latent feature regeneration (He et al., 2024; Bigverdi et al., 2024), and external knowledge integration (Sun et al., 2024; Li et al., 2025a) to improve interoperability. Inspired by the extensive research on the long CoT in LLMs (Guo et al., 2025a), RL-based reasoning approaches have been increasingly explored in MLLMs (Meng et al., 2025; Peng et al., 2025; Shen et al., 2025). These methods predominantly extend text-only reasoning capabilities to a range of multimodal tasks such as spatial reasoning (Zhou et al., 2025), object recognition (Liu et al., 2025b), semantic segmentation (Liu et al., 2025a), and video tasks (Zhao et al., 2025a;b). Unlike methods that hard-code pipelines or simply extend text-only CoT, our approach lets the model autonomously decide when and how to use visual input. Guided by outcome rewards, it adapts visual exploration for a more flexible reasoning process.

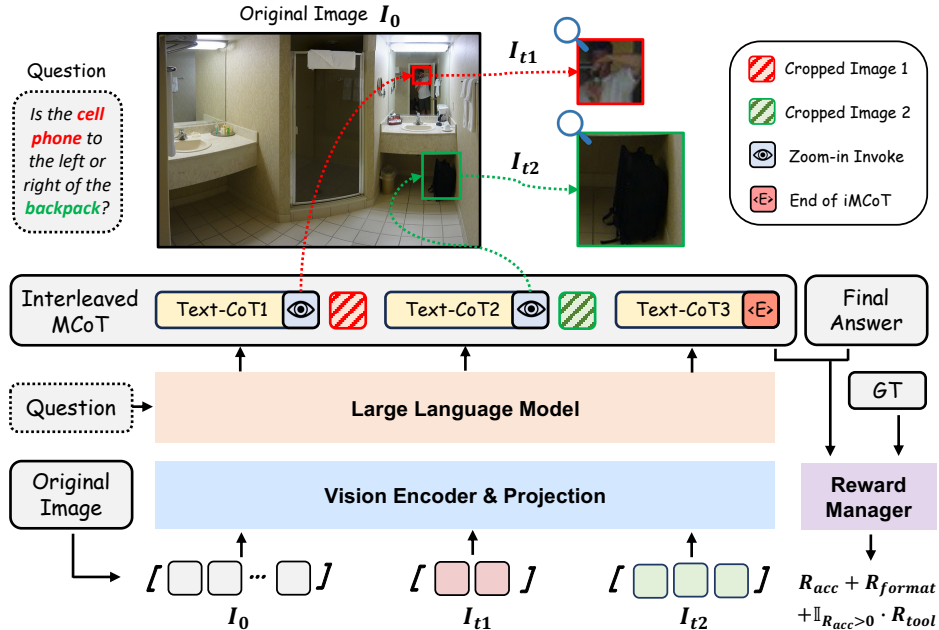


Figure 2: **Overview of DeepEyes.** Our model itself decides whether to perform a second perception via zoom-in by generating grounding coordinates and cropping relevant regions, or to answer directly.

3 METHOD

3.1 DEEPEYES

DeepEyes is a unified multimodal large language model that is capable of “thinking with images” through an iMCoT reasoning process. The ability is inherited from the model’s native capability of visual grounding and action decision planning, and further incentivized and enhanced via end-to-end RL training using outcome reward signals, eliminating the need for cold-start supervised fine-tuning.

As illustrated in Figure 2, given a user question and an image I_0 as input, *DeepEyes* can autonomously decide, after each textual CoT reasoning step, whether to answer directly or perform an image zoom-in for further inspection. The zoom-in operation takes a list of bounding box coordinates as input and outputs the cropped images within the specified regions. The returned crops, such as I_{t1} and I_{t2} , are appended to the ongoing trajectory, enabling the model to reason over all previous context. *DeepEyes* can perform active perception as many times as needed before concluding a final answer. This iterative interaction enables fine-grained perception, especially when the relevant object in the image is small, blurry, or difficult to recognize. During the RL training stage, the reward optimization policy gradient is applied to the entire trajectory, allowing all textual CoTs and action decision planning to be jointly optimized in an end-to-end manner.

Compared to previous works based on workflows or pure text reasoning, our iMCoT offers several significant advantages. (1) **Simplicity in Training.** Previous workflow-based methods Wu & Xie (2024); Li et al. (2025b) depend on substantial SFT data, which is challenging to acquire, while our iMCoT only requires question-answer pairs, reducing data collection complexity. (2) **Enhanced Generalizability.** Workflow-based models are constrained by their task-specific manual design, which hinders their generalization to other tasks. In contrast, our iMCoT exhibits robust generalization capabilities as it learns to dynamically select optimal reasoning processes across diverse tasks through reinforcement learning. (3) **Global Optimization.** Our iMCoT enables joint optimization through end-to-end training, which allows the system to be optimized towards a global optimum. In contrast, optimizing each component separately typically leads to sub-optimal performance. (4) **Multimodal Integration.** Compared to pure text-based thinking, our iMCoT naturally interleaves visual and textual information, combining visual elements with textual reasoning to achieve more accurate perceptual decision-making. (5) **Native Tool Calling.** We encapsulate the model’s native grounding

capability as an internal tool to enable active perception, allowing implicit optimization that previous external-tool paradigms cannot achieve.

3.2 AGENTIC REINFORCEMENT LEARNING

Rollout Formulation. In traditional RL with text-only CoT, the Markov Decision Process (MDP) defines the state as the input prompt tokens together with all tokens generated by the model up to the current step. The action is defined as the next token in the sequence. In contrast, agentic RL extends this formulation by introducing observation tokens, which come from external function calls rather than the model itself. These observation tokens are appended to the ongoing rollout sequence and fed back into the model as input for the subsequent step. We formalize the MDP definition for iMCoT as follows. At each step t , the state s_t of iMCoT is defined as:

$$s_t = \{(X_0, I_0), (X_1, I_1), \dots, (X_t, I_t)\} = \{\mathbf{X}_{\leq t}; \mathbf{I}_{\leq t}\}, \quad (1)$$

where $\mathbf{X}_{\leq t} = \{X_1, \dots, X_t\}$ represents the accumulated sequence of text tokens before step t , and $\mathbf{I}_{\leq t} = \{I_1, \dots, I_t\}$ represents the image observation tokens before step t . We omit other related special tokens that are not generated by VLM itself for simplicity. Given the state s_t , the action $a_t \sim \pi_\theta(a | s_t)$ is sampled from the VLM policy π_θ , serving as the next input token. This iMCoT continues to interleave until either an answer is generated or the maximum number of active perceptions is reached. Note that text tokens $\mathbf{X}_{\leq t}$ and image tokens $\mathbf{I}_{\leq t}$ are interleaved in the states.

Reward Design. In multimodal environments, sparse, outcome-driven rewards are essential for guiding vision-language models toward effective reasoning and decision-making. Because intermediate visual actions lack step-level supervision, we evaluate the entire reasoning trajectory based on the final outcome and the presence of meaningful active perception.

The total reward consists of three parts: an accuracy reward R_{acc} , a format reward R_{format} , and a conditional bonus R_{tool} . Accuracy measures whether the final answer is correct, while formatting penalizes poorly structured outputs. The conditional bonus is granted only when the answer is correct and at least one active perception step is triggered:

$$R(\tau) = R_{\text{acc}}(\tau) + R_{\text{format}}(\tau) + \mathbb{I}_{R_{\text{acc}}(\tau) > 0} R_{\text{tool}}(\tau), \quad (2)$$

where $\mathbb{I}_{R_{\text{acc}}(\tau) > 0}$ equals 1 if the accuracy reward is positive. Conditioning this bonus on a correct answer promotes perception-aware reasoning while discouraging unnecessary actions (see Section 4.3).

Optimization. We adopt Group Relative Policy Optimization (GRPO) (Shao et al., 2024b), which has been proven to be effective for diverse tasks. For multi-turn reasoning trajectories, we apply a token-wise loss mask to ignore loss on observation tokens not generated by the model.

3.3 TRAINING DATA CURATION

A key challenge in training our model via RL is ensuring initial sampling efficiency without an SFT cold start. To address this, we designed a data curation strategy to construct a corpus that is both diverse and specifically targeted to bootstrap effective active perception behavior from the outset.

Data Collection. To construct a robust training corpus, we combine three complementary sources targeting key capabilities: the V^* training set (Wu & Xie, 2024) for fine-grained perception, chart data from ArxivQA (Li et al., 2024b) for task and image diversity, and the ThinkLite-VL (Wang et al., 2025b) dataset to strengthen challenging reasoning. This combination provides a multifaceted foundation for our iMCoT framework, with further details available in Appendix B.

Data Selection. We employ a multi-stage filtering pipeline to curate a dataset aimed at strengthening grounding-assisted visual reasoning. The process begins with *difficulty curation*, where we use Qwen2.5-VL-7B (Bai et al., 2025) to assess question difficulty, removing samples that are either too trivial (100% Acc.) or overly challenging (0% Acc.). Next, we standardize all questions into an open-ended format and perform *data verification* to eliminate incorrectly labeled samples. The final stage applies a *perception-utility filter*, retaining only samples solvable via active perception with ground-truth regions, thereby maximizing informational gain and boosting initial RL sampling efficiency without an SFT cold start. This last filter is applied only to the fine-grained perception data; chart and general reasoning data are preserved in their original, rigorously processed form. The resulting dataset is well-suited for training models with strong interleaved reasoning capabilities.

Table 1: **Results on High-Resolution Benchmarks.** E2E indicates whether the model is end-to-end, requiring no manually defined workflow. * denotes reproduced results.

Model	E2E	Param Size	Attr	V* Bench			HR-Bench 4K			HR-Bench 8K		
				Spatial	Overall		FSP	FCP	Overall	FSP	FCP	Overall
GPT-4o Achiam et al. (2023)	✓	-	-	-	66.0	70.0	48.0	59.0	62.0	49.0	55.5	
o3 OpenAI (2025)	✓	-	-	-	95.7	-	-	-	-	-	-	
SEAL Wu & Xie (2024)	✗	7B	74.8	76.3	75.4	-	-	-	-	-	-	
DyFo Li et al. (2025b)	✗	7B	80.0	82.9	81.2	-	-	-	-	-	-	
ZoomEye Shen et al. (2024a)	✗	7B	93.9	85.5	90.6	84.3	55.0	69.6	88.5	50.0	69.3	
LLaVA-OneVision Li et al. (2024a)	✓	7B	75.7	75.0	75.4	72.0	54.0	63.0	67.3	52.3	59.8	
Qwen2.5-VL* Bai et al. (2025)	✓	7B	73.9	67.1	71.2	85.2	52.2	68.8	78.8	51.8	65.3	
Pixel-Reasoner Su et al. (2025)	✓	7B	83.5	76.3	80.6	86.0	60.3	72.9	80.0	54.3	66.9	
Qwen2.5-VL* Bai et al. (2025)	✓	32B	87.8	88.1	87.9	89.8	58.0	73.9	84.5	56.3	70.4	
DeepEyes	✓	7B	91.3	88.2	90.1	91.3	59.0	75.1	86.8	58.5	72.6	
Δ (vs Qwen2.5-VL 7B)	-	-	+17.4	+21.1	+18.9	+6.1	+6.8	+6.3	+10.0	+6.8	+7.3	

Table 2: **Results on General Perception and Reasoning Benchmark MME-RealWorld-Lite.**

Model	Param Size	Overall	Perception					Reasoning			
			OCR	RS	DT	MO	AD	OCR	DT	MO	AD
LLaVA-OneVision Li et al. (2024a)	7B	43.7	80.0	40.0	56.0	31.7	39.4	65.0	33.0	38.0	32.0
Qwen2.5-VL Bai et al. (2025)	7B	42.3	87.6	32.7	83.0	27.3	30.0	72.0	62.0	28.7	23.0
Qwen2.5-VL Bai et al. (2025)	32B	45.6	87.2	40.7	83.0	29.5	40.7	74.0	60.0	27.3	29.5
Pixel-Reasoner Su et al. (2025)	7B	49.7	89.6	52.0	86.0	38.9	30.9	71.0	72.0	46.0	32.5
DeepEyes	7B	53.2	90.0	52.7	89.0	43.3	33.4	76.0	69.0	44.0	35.0
Δ (vs Qwen2.5-VL 7B)	-	+10.9	+2.4	+20.0	+6.0	+16.0	+3.4	+4.0	+7.0	+15.3	+12.0

Table 3: **Results on Grounding and Hallucination Benchmarks.** * denotes reproduced results.

Model	Param Size	refCOCO	refCOCO+	refCOCog	ReasonSeg	POPE			
						Adversarial	Popular	Random	Overall
LLaVA-OneVision Li et al. (2024a)	7B	-	-	-	-	-	-	-	88.4
Qwen2.5-VL Bai et al. (2025)	7B	90.0	84.2	87.2	-	-	-	-	-
Qwen2.5-VL* Bai et al. (2025)	7B	89.1	82.6	86.1	68.3	85.9	86.5	87.2	85.9
DeepEyes	7B	89.8	83.6	86.7	68.6	84.0	87.5	91.8	87.7
Δ (vs Qwen2.5-VL 7B)	-	+0.7	+1.0	+0.6	+0.3	-1.9	+1.0	+4.6	+1.8

Table 4: **Results on Challenging Reasoning Benchmarks.** * denotes reproduced results, and † denotes results taken from (Zhu et al., 2025).

Model	Param Size	MathVista	MathVerse	MathVision	WeMath	DynaMath	LogicVista
LLaVA-OneVision Li et al. (2024a)	7B	58.6 [†]	19.3 [†]	18.3 [†]	20.9 [†]	-	33.3 [†]
Qwen2.5-VL Bai et al. (2025)	7B	68.2	49.2	25.1	35.2 [†]	-	44.1 [†]
Qwen2.5-VL* Bai et al. (2025)	7B	68.3	45.6	25.6	34.6	53.3	45.9
DeepEyes	7B	70.1	47.3	26.6	38.9	55.0	47.7
Δ (vs Qwen2.5-VL 7B)	-	+1.9	+1.7	+1.0	+4.3	+1.7	+1.8

4 EXPERIMENT

4.1 SETUPS

Baselines and Benchmarks. To comprehensively assess the effectiveness of *DeepEyes*, we compare it against three categories of baselines: (1) advanced *proprietary* models, including OpenAI GPT-4o (Achiam et al., 2023) and o3 (OpenAI, 2025); (2) state-of-the-art *open-source* models, such as LLaVA-OneVision (Li et al., 2024a) and Qwen2.5-VL (Bai et al., 2025); and (3) approaches explicitly designed with *workflows*, such as SEAL (Wu & Xie, 2024), DyFo (Li et al., 2025b) and ZoomEye (Shen et al., 2024a). Since tasks requiring fine-grained visual understanding naturally highlight the strengths of iMCoT, we first evaluate *DeepEyes* on high-resolution benchmarks. Then, we assess *DeepEyes* on grounding and hallucination benchmarks to show improvements brought by iMCoT on general visual capabilities. We also adopt general reasoning benchmarks to verify its effectiveness.

Training Details. We train Qwen2.5-VL-7B with GRPO for 80 iterations on H100 GPUs. Each batch samples 256 prompts, with 16 rollouts per prompt, up to a maximum of 6 times of active perceptions. We set the KL coefficient to 0.0 and define the maximum response length as 20480 tokens.

4.2 MAIN RESULTS

High-Resolution Benchmarks. High-resolution benchmarks, such as V^* (Wu & Xie, 2024) and HR-Bench (Wang et al., 2025a), contain very large images (2K–8K) with small target objects, making accurate localization challenging for VLMs. As shown in Table 1, our model significantly outperforms existing open-source methods, including complex pipelines (Wu & Xie, 2024; Li et al., 2025b; Shen et al., 2024a), achieving 18.9% and 7.3% gains over Qwen2.5-VL 7B on V^* and HR-Bench 8K, respectively. This demonstrates that simple RL can effectively unlock high-resolution visual reasoning without elaborate pipelines.

General Perception and Reasoning Benchmark. As shown in Table 2, our 7B model delivers top performance on MME-RealWorld-Lite (Zhang et al., 2024b). It surpasses both the 7B and even 32B versions of Qwen2.5-VL, demonstrating superior real-world perception and reasoning.

Grounding and Hallucination Benchmarks. Furthermore, the multimodal CoT enhances general visual capabilities. Evaluated on grounding (refCOCO/refCOCO+ (Caesar et al., 2018), refCOCOg (Kazemzadeh et al., 2014), ReasonSeg (Lai et al., 2024)) and hallucination (POPE (Li et al., 2023c)) benchmarks, our model achieves higher grounding accuracy and substantially reduces hallucinations (Table 3). This improvement stems from our model’s ability to focus on regions of interest during visual reasoning and analyze cropped areas in detail, enabling more confident verification of object presence. These results show that iMCoT not only boosts high-resolution perception but also enhances overall visual reliability with a more thorough verification mechanism.

Challenging Reasoning Benchmarks. We further evaluate our model on MathVista (Lu et al., 2023), MathVerse (Zhang et al., 2024a), MathVision (Wang et al., 2024a), WeMath (Qiao et al., 2024), DynaMath (Zou et al., 2024), and LogicVista (Xiao et al., 2024) in Table 4. Benefiting from the integrated chain-of-thought mechanism, our model achieves consistent performance improvements across these challenging multimodal reasoning benchmarks, including mathematical problem-solving.

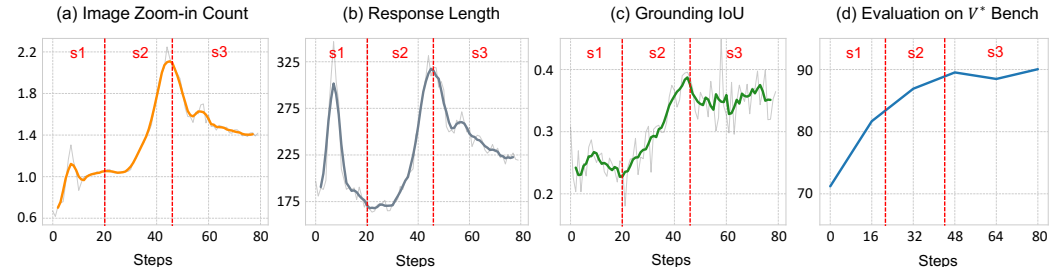


Figure 3: Training dynamics of *DeepEyes* on V^* . s1/2/3 represent different stages.

4.3 KEY FINDINGS: FROM CASUAL USER TO PROFICIENT VISUAL REASONER

Training Dynamics. To better understand the model’s behavior during end-to-end reinforcement learning, we analyze its performance on fine-grained data V^* . Since fine-grained data includes ground-truth bounding boxes closely aligned with target answers, we quantify the quality of the model’s visual grounding using Intersection-over-Union (IoU). In Figure 3, a clear evolution emerges in how the model leverages active perception. This progression unfolds in three stages, reflecting increasingly effective integration of active perception into reasoning:

- **Stage 1: Initial Exploration (Steps 0–20)** The model starts following system prompts to access additional visual cues, but lacks a coherent strategy. Action count and response length rise, reflecting exploratory behavior, while low grounding IoU shows repeated attempts without successfully linking retrieved information to the visual context. A sharp drop in response length between steps 8 and 20 indicates it is streamlining descriptions while acquiring basic active perception skills.
- **Stage 2: High-Frequency Engagement (Steps 20–45)** The model enters a phase of intensive active perception, repeatedly leveraging visual information to boost accuracy and reward. Key metrics, including grounding IoU, improve, while longer responses and frequent visual interactions suggest a “broad sweep” strategy: the model externalizes reasoning by over-querying the environment. This stage reflects growing recognition of active perception’s value, though efficiency remains suboptimal.

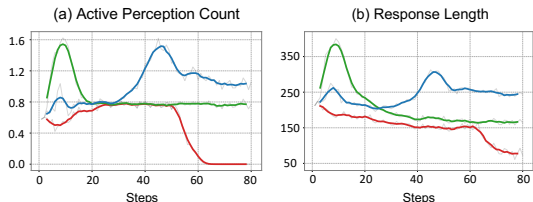


Figure 4: Training dynamics w.r.t. tool reward.

Table 6: **Scaling Model Size.** The 32B model is trained with the same data. Resp. Len.: Average Response Length. IoU is measured on V^* .

Model	V^*	WeMath	Resp. Len.	IoU
Qwen2.5-VL-7B	71.2	34.6	212	-
DeepEyes-7B	90.1	38.9	241	0.37
Qwen2.5-VL-32B	87.9	47.7	314	-
DeepEyes-32B	93.3	55.9	754	0.53

Table 8: **Zero-Shot Tool Generalization.** HR-OCR-Rot: Random rotated subsets of HR-Bench-8K for OCR tasks.

Model	V^*	HR-OCR-Rot
Qwen2.5-VL-7B	71.2	76.5
DeepEyes (crop)	90.1	80.1
DeepEyes (crop+rotate)	90.1	83.6

Table 5: Evaluations w.r.t. tool reward.

Method	V^*	HR-4k	HR-8k
w/o Tool Reward	87.4	53.4	55.4
Unconditional Reward	87.4	72.1	71.8
Conditional Reward	90.1	75.1	72.6

Table 7: **Scaling Challenging Reasoning Data** from Chen et al. (2025) shows co-evolving perception (V^*) and mathematical problem-solving.

Model	MVerse	WeMath	V^*
Qwen2.5-VL-7B	45.6	34.6	71.2
DeepEyes-7B	47.3	38.9	90.1
+ More Reasoning Data	51.8	43.6	91.6

Table 9: **Ablation on iMCoT.** We provide results trained with text-only CoT on the same datasets.

Model	V^*	HR-4K	HR-8K
Qwen2.5-VL-7B	71.2	68.8	65.3
RL w. Text-only CoT	88.5	75.4	60.8
DeepEyes (iMCoT)	90.1	75.1	72.6

• **Stage 3: Efficient Utilization (Steps 45–80)** The model adopts a more selective, precise approach, reducing query frequency and response length while maintaining high grounding and task accuracy. This reveals a compact visual-linguistic policy: active perception is invoked only when needed, complementing internal reasoning. High IoU with fewer queries reflects implicit planning, as the model narrows the visual scope internally before selectively confirming hypotheses.

Overall, training progresses from broad exploration to targeted exploitation, showing that the model can learn to integrate active perception into reasoning effectively. The ability to leverage active perception strategically co-evolves with its policy, highlighting the potential of perception-augmented visual-language models for scalable and interpretable multimodal reasoning.

Tool Reward. The reward in Eq. 2 includes a conditional component (*tool reward*) that grants a bonus only when the model answers correctly while performing active perceptions. For comparison, we train two variants: one without the conditional bonus (*w/o tool reward*) and one with an unconditional bonus (*unconditional reward*). Results are shown in Figure 4 and Table 5. Without the conditional reward, the model quickly reduces and stops performing perception actions. With an unconditional bonus, minimal engagement persists but remains static. Conditioning the reward on correctness leads to gradually increased active perceptions and more informative responses, reflecting deeper integration of visual reasoning. This setting achieves the highest accuracy, showing that rewarding actions alone are insufficient; alignment with correct outcomes is essential in *DeepEyes*.

Thinking Patterns. Here, we analyze diverse thinking patterns that emerged during end-to-end RL training, showing how the model performs active perceptions into its reasoning in ways that mirror human visual cognition. Four primary patterns can be identified: **1) Visual Search:** When facing complex problems that a single observation can’t solve, the model actively scans different image regions, gathers visual clues, and reasons through them to reach reliable conclusions (Figure 7); **2) Visual Comparison:** When handling understanding across multiple images or objects, the model iteratively zooms in on each one, allowing close examination and comparison before drawing a final conclusion (Figure 8); **3) Visual Confirmation:** In some cases, the model begins with uncertainty but gradually builds confidence by zooming in on image details to gather evidence and resolve doubts (Figure 9); **4) Hallucination Mitigation:** Although VLMs can sometimes hallucinate, performing active perceptions helps the model focus on visual details to mitigate hallucination. (Figure 10).

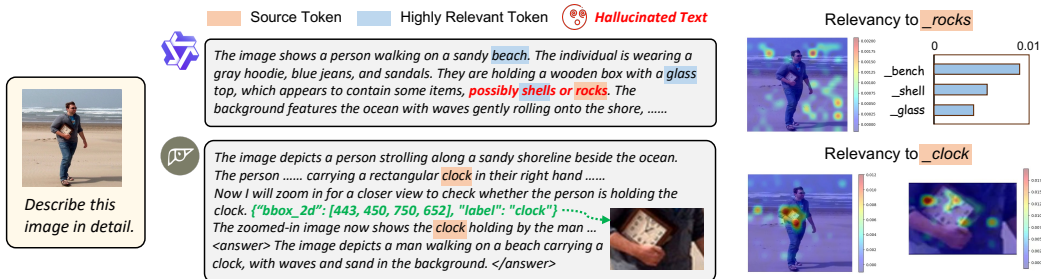


Figure 5: Analysis of hallucination mitigation. Qwen2.5-VL-7B (top) hallucinates “rocks,” driven by linguistic association with “beach” rather than visual evidence, yielding low relevancy. In contrast, *DeepEyes* (bottom) triggers iMCoT to counter this bias, zooming in to re-ground reasoning and override the language prior, correctly identifying the “clock” with a focused relevancy heatmap.

4.4 ANALYSIS AND ABLATION STUDY

Scaling Model Size. Our framework exhibits strong scalability, as evidenced in Table 6. When scaling from 7B to 32B parameters, *DeepEyes* consistently widens its performance gap over the Qwen2.5-VL baseline. More importantly, the larger model demonstrates more sophisticated emergent behaviors. It generates substantially longer reasoning chains (Resp. Len.) and achieves higher grounding precision (IoU). This indicates that our RL paradigm not only boosts task performance but also fosters deeper and more accurate reasoning as model capacity increases.

Scaling Challenging Reasoning Data. As shown in Table 7, scaling our training set with more challenging reasoning data (from 23% to 42%) demonstrates a mutual reinforcement between perception and reasoning, improving performance on both mathematical benchmarks and the perception task V^* as well. We hypothesize that stronger abstract reasoning enables a more sophisticated understanding of complex queries, which in turn guides a more effective visual-grounded thinking process.

Zero-Shot Tool Generalization. The primary goal of *DeepEyes* is to explore how models can natively “think with images,” using cropping as a simple, foundational tool. Although not aimed at building a large toolset, the framework is easily extensible. To verify this, we introduced a *rotate* tool solely through the system prompt, requiring no retraining or architectural changes. We evaluated it on HR-OCR-Rot, a benchmark we created by applying random rotations ($0^\circ, 90^\circ, 180^\circ, 270^\circ$) to the HRBench-8K OCR subset. As shown in Table 8, the tool yielded a 3.5% performance gain on this task while maintaining stable results on the general V^* benchmark, demonstrating that *DeepEyes* can seamlessly integrate new tools and apply them selectively for zero-shot generalization.

Ablation on iMCoT. Finally, the ablation in Table 9 isolates the contribution of our core iMCoT mechanism. Compared to an RL baseline trained with a text-only CoT, iMCoT achieves superior performance across all benchmarks. The advantage is most pronounced on the ultra-high-resolution HR-8K benchmark, where iMCoT outperforms the text-only approach by a substantial margin. This result decisively demonstrates that for tasks requiring fine-grained visual detail, interleaving visual perception with textual reasoning is not merely beneficial, but essential for robust performance.

4.5 CASE STUDY: HOW DOES *DeepEyes* SYSTEMATICALLY MITIGATE HALLUCINATION?

Object hallucination in VLMs often stems from a strong language bias (Zhou et al., 2024), where text generation detaches from the visual input to rely on learned linguistic patterns. Our “thinking with images” paradigm directly counters this. By triggering active perception, the model is forced to re-engage with visual evidence, effectively fact-checking its linguistic assumptions against visual reality. To analyze this mechanism, we compute *relevancy maps* (Ben Melech Stan et al., 2024) to quantify the grounding of the model’s output, which measures the contribution of all preceding tokens to the generation of a specific source token. Visualized via heatmaps, high relevancy attributed to image regions indicates strong visual grounding, whereas high relevancy from purely textual priors suggests a language-driven hallucination. As illustrated in Figure 5, this approach proves effective. While a baseline model succumbs to linguistic bias, *DeepEyes* leverages active perception to re-evaluate its initial assumptions based on new visual evidence. This process breaks ungrounded reasoning, overriding the language prior and correcting the hallucination, as confirmed by our relevancy analysis.

5 CONCLUSION

In this paper, we presented *DeepEyes*, a vision-language model that learns to “think with images” via end-to-end reinforcement learning. Unlike prior methods, this capability emerges natively, requiring neither pre-collected reasoning data for SFT nor external specialized models. To guide its reasoning behavior, we propose an active perception mechanism, featuring tailored data selection and rewards, that promotes successful reasoning trajectories by incentivizing the strategic use of visual grounding. Consequently, *DeepEyes* achieves competitive results on multiple benchmarks, exhibiting diverse, human-like reasoning patterns such as visual search and comparison.

LLM USAGE STATEMENT

LLMs were used solely for grammar and language polishing; all ideas, analyses, and writing were produced entirely by the authors.

REPRODUCIBILITY STATEMENT

Code is available at <https://github.com/Visual-Agent/DeepEyes>. It includes comprehensive setup instructions, training scripts, and documentation to facilitate easy reproduction of our experiments.

REFERENCES

- Josh Achiam, Steven Adler, Sandhini Agarwal, Lama Ahmad, Ilge Akkaya, Florencia Leoni Aleman, Diogo Almeida, Janko Altenschmidt, Sam Altman, Shyamal Anadkat, et al. Gpt-4 technical report. *arXiv preprint arXiv:2303.08774*, 2023.
- Jean-Baptiste Alayrac, Jeff Donahue, Pauline Luc, Antoine Miech, Iain Barr, Yana Hasson, Karel Lenc, Arthur Mensch, Katherine Millican, Malcolm Reynolds, et al. Flamingo: a visual language model for few-shot learning. *Advances in neural information processing systems*, 35:23716–23736, 2022.
- Jinze Bai, Shuai Bai, Yunfei Chu, Zeyu Cui, Kai Dang, Xiaodong Deng, Yang Fan, Wenbin Ge, Yu Han, Fei Huang, et al. Qwen technical report. *arXiv preprint arXiv:2309.16609*, 2023.
- Shuai Bai, Keqin Chen, Xuejing Liu, Jialin Wang, Wenbin Ge, Siboz Song, Kai Dang, Peng Wang, Shijie Wang, Jun Tang, et al. Qwen2. 5-vl technical report. *arXiv preprint arXiv:2502.13923*, 2025.
- Gabriela Ben Melech Stan, Estelle Aflalo, Raanan Yehezkel Rohekar, Anahita Bhiwandiwalla, Shao-Yen Tseng, Matthew Lyle Olson, Yaniv Gurwicz, Chenfei Wu, Nan Duan, and Vasudev Lal. Lvlm-intrepret: An interpretability tool for large vision-language models. In *CVPR*, pp. 8182–8187, 2024.
- Mahtab Bigverdi, Zelun Luo, Cheng-Yu Hsieh, Ethan Shen, Dongping Chen, Linda G Shapiro, and Ranjay Krishna. Perception tokens enhance visual reasoning in multimodal language models. *arXiv preprint arXiv:2412.03548*, 2024.
- Holger Caesar, Jasper Uijlings, and Vittorio Ferrari. Coco-stuff: Thing and stuff classes in context. In *Proceedings of the IEEE conference on computer vision and pattern recognition*, pp. 1209–1218, 2018.
- Kezhen Chen, Rahul Thapa, Rahul Chalamala, Ben Athiwaratkun, Shuaiwen Leon Song, and James Zou. Dragonfly: Multi-resolution zoom supercharges large visual-language model. *arXiv e-prints*, pp. arXiv–2406, 2024a.
- Shuang Chen, Yue Guo, Zhaochen Su, Yafu Li, Yulun Wu, Jiacheng Chen, Jiayu Chen, Weijie Wang, Xiaoye Qu, and Yu Cheng. Advancing multimodal reasoning: From optimized cold start to staged reinforcement learning. *arXiv preprint arXiv:2506.04207*, 2025.

- Zhe Chen, Weiyun Wang, Yue Cao, Yangzhou Liu, Zhangwei Gao, Erfei Cui, Jinguo Zhu, Shenglong Ye, Hao Tian, Zhaoyang Liu, et al. Expanding performance boundaries of open-source multimodal models with model, data, and test-time scaling. *arXiv preprint arXiv:2412.05271*, 2024b.
- Zhe Chen, Jiannan Wu, Wenhai Wang, Weijie Su, Guo Chen, Sen Xing, Muyan Zhong, Qinglong Zhang, Xizhou Zhu, Lewei Lu, et al. Internvl: Scaling up vision foundation models and aligning for generic visual-linguistic tasks. In *Proceedings of the IEEE/CVF conference on computer vision and pattern recognition*, pp. 24185–24198, 2024c.
- Xingyu Fu, Minqian Liu, Zhengyuan Yang, John Corring, Yijuan Lu, Jianwei Yang, Dan Roth, Dinei Florencio, and Cha Zhang. Refocus: Visual editing as a chain of thought for structured image understanding. *arXiv preprint arXiv:2501.05452*, 2025.
- Zhangwei Gao, Zhe Chen, Erfei Cui, Yiming Ren, Weiyun Wang, Jinguo Zhu, Hao Tian, Shenglong Ye, Junjun He, Xizhou Zhu, et al. Mini-internvl: a flexible-transfer pocket multi-modal model with 5% parameters and 90% performance. *Visual Intelligence*, 2(1):1–17, 2024.
- Daya Guo, Dejian Yang, Haowei Zhang, Junxiao Song, Ruoyu Zhang, Runxin Xu, Qihao Zhu, Shirong Ma, Peiyi Wang, Xiao Bi, et al. Deepseek-r1: Incentivizing reasoning capability in llms via reinforcement learning. *arXiv preprint arXiv:2501.12948*, 2025a.
- Dong Guo, Faming Wu, Feida Zhu, Fuxing Leng, Guang Shi, Haobin Chen, Haoqi Fan, Jian Wang, Jianyu Jiang, Jiawei Wang, et al. Seed1. 5-vl technical report. *arXiv preprint arXiv:2505.07062*, 2025b.
- Zonghao Guo, Ruyi Xu, Yuan Yao, Junbo Cui, Zanlin Ni, Chunjiang Ge, Tat-Seng Chua, Zhiyuan Liu, and Gao Huang. Llava-uhd: an llm perceiving any aspect ratio and high-resolution images. In *European Conference on Computer Vision*, pp. 390–406. Springer, 2024.
- Liqi He, Zuchao Li, Xiantao Cai, and Ping Wang. Multi-modal latent space learning for chain-of-thought reasoning in language models. In *Proceedings of the AAAI Conference on Artificial Intelligence*, volume 38, pp. 18180–18187, 2024.
- Sahar Kazemzadeh, Vicente Ordonez, Mark Matten, and Tamara Berg. Referitgame: Referring to objects in photographs of natural scenes. In *Proceedings of the 2014 conference on empirical methods in natural language processing (EMNLP)*, pp. 787–798, 2014.
- Xin Lai, Zhuotao Tian, Yukang Chen, Yanwei Li, Yuhui Yuan, Shu Liu, and Jiaya Jia. Lisa: Reasoning segmentation via large language model. In *Proceedings of the IEEE/CVF Conference on Computer Vision and Pattern Recognition*, pp. 9579–9589, 2024.
- Bo Li, Yuanhan Zhang, Dong Guo, Renrui Zhang, Feng Li, Hao Zhang, Kaichen Zhang, Peiyuan Zhang, Yanwei Li, Ziwei Liu, et al. Llava-onevision: Easy visual task transfer. *arXiv preprint arXiv:2408.03326*, 2024a.
- Chengzu Li, Wenshan Wu, Huanyu Zhang, Yan Xia, Shaoguang Mao, Li Dong, Ivan Vulić, and Furu Wei. Imagine while reasoning in space: Multimodal visualization-of-thought. *arXiv preprint arXiv:2501.07542*, 2025a.
- Chunyuan Li, Cliff Wong, Sheng Zhang, Naoto Usuyama, Haotian Liu, Jianwei Yang, Tristan Naumann, Hoifung Poon, and Jianfeng Gao. Llava-med: Training a large language-and-vision assistant for biomedicine in one day. *Advances in Neural Information Processing Systems*, 36: 28541–28564, 2023a.
- Geng Li, Jinglin Xu, Yunzhen Zhao, and Yuxin Peng. Dyfo: A training-free dynamic focus visual search for enhancing llms in fine-grained visual understanding. *arXiv preprint arXiv:2504.14920*, 2025b.
- Junnan Li, Dongxu Li, Silvio Savarese, and Steven Hoi. Blip-2: Bootstrapping language-image pre-training with frozen image encoders and large language models. In *International conference on machine learning*, pp. 19730–19742. PMLR, 2023b.

- Lei Li, Yuqi Wang, Runxin Xu, Peiyi Wang, Xiachong Feng, Lingpeng Kong, and Qi Liu. Multimodal arxiv: A dataset for improving scientific comprehension of large vision-language models. In *Proceedings of the 62nd Annual Meeting of the Association for Computational Linguistics (Volume 1: Long Papers)*, pp. 14369–14387, 2024b.
- Yifan Li, Yifan Du, Kun Zhou, Jinpeng Wang, Wayne Xin Zhao, and Ji-Rong Wen. Evaluating object hallucination in large vision-language models. *arXiv preprint arXiv:2305.10355*, 2023c.
- Yunxin Li, Shenyuan Jiang, Baotian Hu, Longyue Wang, Wanqi Zhong, Wenhan Luo, Lin Ma, and Min Zhang. Uni-moe: Scaling unified multimodal llms with mixture of experts. *IEEE Transactions on Pattern Analysis and Machine Intelligence*, 2025c.
- Bin Lin, Yang Ye, Bin Zhu, Jiayi Cui, Munan Ning, Peng Jin, and Li Yuan. Video-llava: Learning united visual representation by alignment before projection. *arXiv preprint arXiv:2311.10122*, 2023.
- Tsung-Yi Lin, Michael Maire, Serge Belongie, James Hays, Pietro Perona, Deva Ramanan, Piotr Dollár, and C Lawrence Zitnick. Microsoft coco: Common objects in context. In *Computer vision—ECCV 2014: 13th European conference, zurich, Switzerland, September 6-12, 2014, proceedings, part v 13*, pp. 740–755. Springer, 2014.
- Haotian Liu, Chunyuan Li, Yuheng Li, and Yong Jae Lee. Improved baselines with visual instruction tuning, 2023a.
- Haotian Liu, Chunyuan Li, Qingyang Wu, and Yong Jae Lee. Visual instruction tuning. In *NeurIPS*, 2023b.
- Haotian Liu, Chunyuan Li, Yuheng Li, Bo Li, Yuanhan Zhang, Sheng Shen, and Yong Jae Lee. Lllavanext: Improved reasoning, ocr, and world knowledge, 2024a.
- Shilong Liu, Hao Cheng, Haotian Liu, Hao Zhang, Feng Li, Tianhe Ren, Xueyan Zou, Jianwei Yang, Hang Su, Jun Zhu, et al. Llava-plus: Learning to use tools for creating multimodal agents. In *European Conference on Computer Vision*, pp. 126–142. Springer, 2024b.
- Yuqi Liu, Bohao Peng, Zhisheng Zhong, Zihao Yue, Fanbin Lu, Bei Yu, and Jiaya Jia. Seg-zero: Reasoning-chain guided segmentation via cognitive reinforcement. *arXiv preprint arXiv:2503.06520*, 2025a.
- Ziyu Liu, Zeyi Sun, Yuhang Zang, Xiaoyi Dong, Yuhang Cao, Haodong Duan, Dahua Lin, and Jiaqi Wang. Visual-rft: Visual reinforcement fine-tuning. *arXiv preprint arXiv:2503.01785*, 2025b.
- Zuyan Liu, Yuhao Dong, Yongming Rao, Jie Zhou, and Jiwen Lu. Chain-of-spot: Interactive reasoning improves large vision-language models. *arXiv preprint arXiv:2403.12966*, 2024c.
- Dongchen Lu, Yuyao Sun, Zilu Zhang, Leping Huang, Jianliang Zeng, Mao Shu, and Huo Cao. Internvl-x: Advancing and accelerating internvl series with efficient visual token compression. *arXiv preprint arXiv:2503.21307*, 2025.
- Pan Lu, Hritik Bansal, Tony Xia, Jiacheng Liu, Chunyuan Li, Hannaneh Hajishirzi, Hao Cheng, Kai-Wei Chang, Michel Galley, and Jianfeng Gao. Mathvista: Evaluating mathematical reasoning of foundation models in visual contexts. *arXiv preprint arXiv:2310.02255*, 2023.
- Xuwen Luo, Fan Ding, Yinsheng Song, Xiaofeng Zhang, and Junnyong Loo. Pkrd-cot: A unified chain-of-thought prompting for multi-modal large language models in autonomous driving. *arXiv preprint arXiv:2412.02025*, 2024.
- Fanqing Meng, Lingxiao Du, Zongkai Liu, Zhixiang Zhou, Quanfeng Lu, Daocheng Fu, Tiancheng Han, Botian Shi, Wenhai Wang, Junjun He, et al. Mm-eureka: Exploring the frontiers of multimodal reasoning with rule-based reinforcement learning. *arXiv preprint arXiv:2503.07365*, 2025.
- Debjyoti Mondal, Suraj Modi, Subhadarshi Panda, Rituraj Singh, and Godawari Sudhakar Rao. Kam-cot: Knowledge augmented multimodal chain-of-thoughts reasoning. In *Proceedings of the AAAI conference on artificial intelligence*, volume 38, pp. 18798–18806, 2024.

- Niklas Muennighoff, Zitong Yang, Weijia Shi, Xiang Lisa Li, Li Fei-Fei, Hannaneh Hajishirzi, Luke Zettlemoyer, Percy Liang, Emmanuel Candès, and Tatsunori Hashimoto. s1: Simple test-time scaling. *arXiv preprint arXiv:2501.19393*, 2025.
- Jiri Najemnik and Wilson S Geisler. Optimal eye movement strategies in visual search. *Nature*, 434 (7031):387–391, 2005.
- OpenAI. Thinking with images. <https://openai.com/index/thinking-with-images/>, 2025.
- Yingzhe Peng, Gongrui Zhang, Miaosen Zhang, Zhiyuan You, Jie Liu, Qipeng Zhu, Kai Yang, Xingzhong Xu, Xin Geng, and Xu Yang. Lmm-r1: Empowering 3b llms with strong reasoning abilities through two-stage rule-based rl. *arXiv preprint arXiv:2503.07536*, 2025.
- Runqi Qiao, Qiuna Tan, Guanting Dong, Minhui Wu, Chong Sun, Xiaoshuai Song, Zhuoma GongQue, Shanglin Lei, Zhe Wei, Miaoxuan Zhang, et al. We-math: Does your large multimodal model achieve human-like mathematical reasoning? *arXiv preprint arXiv:2407.01284*, 2024.
- Stéphane Ross, Geoffrey Gordon, and Drew Bagnell. A reduction of imitation learning and structured prediction to no-regret online learning. In *Proceedings of the fourteenth international conference on artificial intelligence and statistics*, pp. 627–635. JMLR Workshop and Conference Proceedings, 2011.
- Hao Shao, Shengju Qian, Han Xiao, Guanglu Song, Zhuofan Zong, Letian Wang, Yu Liu, and Hongsheng Li. Visual cot: Advancing multi-modal language models with a comprehensive dataset and benchmark for chain-of-thought reasoning. *Advances in Neural Information Processing Systems*, 37:8612–8642, 2024a.
- Zhihong Shao, Peiyi Wang, Qihao Zhu, Runxin Xu, Junxiao Song, Xiao Bi, Haowei Zhang, Mingchuan Zhang, Y. K. Li, Y. Wu, and Daya Guo. Deepseekmath: Pushing the limits of mathematical reasoning in open language models, 2024b. URL <https://arxiv.org/abs/2402.03300>.
- Haozhan Shen, Kangjia Zhao, Tiancheng Zhao, Ruochen Xu, Zilun Zhang, Mingwei Zhu, and Jianwei Yin. Zoomeye: Enhancing multimodal llms with human-like zooming capabilities through tree-based image exploration. *arXiv preprint arXiv:2411.16044*, 2024a.
- Haozhan Shen, Peng Liu, Jingcheng Li, Chunxin Fang, Yibo Ma, Jiajia Liao, Qiaoli Shen, Zilun Zhang, Kangjia Zhao, Qianqian Zhang, et al. Vlm-r1: A stable and generalizable r1-style large vision-language model. *arXiv preprint arXiv:2504.07615*, 2025.
- Leyang Shen, Gongwei Chen, Rui Shao, Weili Guan, and Liqiang Nie. Mome: Mixture of multimodal experts for generalist multimodal large language models. *arXiv preprint arXiv:2407.12709*, 2024b.
- Fangxun Shu, Yue Liao, Le Zhuo, Chenning Xu, Lei Zhang, Guanghao Zhang, Haonan Shi, Long Chen, Tao Zhong, Wangui He, et al. Llava-mod: Making llava tiny via moe knowledge distillation. *arXiv preprint arXiv:2408.15881*, 2024.
- Alex Su, Haozhe Wang, Weiming Ren, Fangzhen Lin, and Wenhui Chen. Pixel reasoner: Incentivizing pixel-space reasoning with curiosity-driven reinforcement learning. *arXiv preprint arXiv:2505.15966*, 2025.
- Guangyan Sun, Mingyu Jin, Zhenting Wang, Cheng-Long Wang, Siqi Ma, Qifan Wang, Tong Geng, Ying Nian Wu, Yongfeng Zhang, and Dongfang Liu. Visual agents as fast and slow thinkers. *arXiv preprint arXiv:2408.08862*, 2024.
- Kimi Team, Angang Du, Bofei Gao, Bofei Xing, Changjiu Jiang, Cheng Chen, Cheng Li, Chenjun Xiao, Chenzhuang Du, Chonghua Liao, et al. Kimi k1. 5: Scaling reinforcement learning with llms. *arXiv preprint arXiv:2501.12599*, 2025a.
- Kimi Team, Angang Du, Bohong Yin, Bofei Xing, Bowen Qu, Bowen Wang, Cheng Chen, Chenlin Zhang, Chenzhuang Du, Chu Wei, et al. Kimi-vl technical report. *arXiv preprint arXiv:2504.07491*, 2025b.

- Ke Wang, Junting Pan, Weikang Shi, Zimu Lu, Houxing Ren, Aojun Zhou, Mingjie Zhan, and Hongsheng Li. Measuring multimodal mathematical reasoning with math-vision dataset. *Advances in Neural Information Processing Systems*, 37:95095–95169, 2024a.
- Peng Wang, Shuai Bai, Sinan Tan, Shijie Wang, Zhihao Fan, Jinze Bai, Keqin Chen, Xuejing Liu, Jialin Wang, Wenbin Ge, et al. Qwen2-vl: Enhancing vision-language model’s perception of the world at any resolution. *arXiv preprint arXiv:2409.12191*, 2024b.
- Wenbin Wang, Liang Ding, Minyan Zeng, Xiabin Zhou, Li Shen, Yong Luo, Wei Yu, and Dacheng Tao. Divide, conquer and combine: A training-free framework for high-resolution image perception in multimodal large language models. In *Proceedings of the AAAI Conference on Artificial Intelligence*, volume 39, pp. 7907–7915, 2025a.
- Xiyao Wang, Zhengyuan Yang, Chao Feng, Hongjin Lu, Linjie Li, Chung-Ching Lin, Kevin Lin, Furong Huang, and Lijuan Wang. Sota with less: Mcts-guided sample selection for data-efficient visual reasoning self-improvement. *arXiv preprint arXiv:2504.07934*, 2025b.
- Yana Wei, Liang Zhao, Kangheng Lin, En Yu, Yuang Peng, Runpei Dong, Jianjian Sun, Haoran Wei, Zheng Ge, Xiangyu Zhang, et al. Perception in reflection. *arXiv preprint arXiv:2504.07165*, 2025.
- Penghao Wu and Saining Xie. V?: Guided visual search as a core mechanism in multimodal llms. In *Proceedings of the IEEE/CVF Conference on Computer Vision and Pattern Recognition*, pp. 13084–13094, 2024.
- Yijia Xiao, Edward Sun, Tianyu Liu, and Wei Wang. Logicvista: Multimodal llm logical reasoning benchmark in visual contexts. *arXiv preprint arXiv:2407.04973*, 2024.
- Jinheng Xie, Weijia Mao, Zechen Bai, David Junhao Zhang, Weihao Wang, Kevin Qinghong Lin, Yuchao Gu, Zhijie Chen, Zhenheng Yang, and Mike Zheng Shou. Show-o: One single transformer to unify multimodal understanding and generation. *arXiv preprint arXiv:2408.12528*, 2024.
- Chenkai Xu, Xu Wang, Zhenyi Liao, Yishun Li, Tianqi Hou, and Zhijie Deng. Show-o turbo: Towards accelerated unified multimodal understanding and generation. *arXiv preprint arXiv:2502.05415*, 2025.
- An Yang, Baosong Yang, Beichen Zhang, Binyuan Hui, Bo Zheng, Bowen Yu, Chengyuan Li, Dayiheng Liu, Fei Huang, Haoran Wei, et al. Qwen2. 5 technical report. *arXiv preprint arXiv:2412.15115*, 2024.
- Zhengyuan Yang, Linjie Li, Kevin Lin, Jianfeng Wang, Chung-Ching Lin, Zicheng Liu, and Lijuan Wang. The dawn of llms: Preliminary explorations with gpt-4v (ision). *arXiv preprint arXiv:2309.17421*, 9(1):1, 2023.
- Jiabo Ye, Haiyang Xu, Haowei Liu, Anwen Hu, Ming Yan, Qi Qian, Ji Zhang, Fei Huang, and Jingren Zhou. mplug-owl3: Towards long image-sequence understanding in multi-modal large language models. *arXiv preprint arXiv:2408.04840*, 2024a.
- Qinghao Ye, Haiyang Xu, Guohai Xu, Jiabo Ye, Ming Yan, Yiyang Zhou, Junyang Wang, Anwen Hu, Pengcheng Shi, Yaya Shi, et al. mplug-owl: Modularization empowers large language models with multimodality. *arXiv preprint arXiv:2304.14178*, 2023.
- Qinghao Ye, Haiyang Xu, Jiabo Ye, Ming Yan, Anwen Hu, Haowei Liu, Qi Qian, Ji Zhang, and Fei Huang. mplug-owl2: Revolutionizing multi-modal large language model with modality collaboration. In *Proceedings of the IEEE/CVF conference on computer vision and pattern recognition*, pp. 13040–13051, 2024b.
- Qiyuan Zhang, Fuyuan Lyu, Zexu Sun, Lei Wang, Weixu Zhang, Zhihan Guo, Yufei Wang, Irwin King, Xue Liu, and Chen Ma. What, how, where, and how well? a survey on test-time scaling in large language models. *arXiv preprint arXiv:2503.24235*, 2025a.
- Renrui Zhang, Dongzhi Jiang, Yichi Zhang, Haokun Lin, Ziyu Guo, Pengshuo Qiu, Aojun Zhou, Pan Lu, Kai-Wei Chang, Yu Qiao, et al. Mathverse: Does your multi-modal llm truly see the diagrams in visual math problems? In *European Conference on Computer Vision*, pp. 169–186. Springer, 2024a.

- Shaolei Zhang, Qingkai Fang, Zhe Yang, and Yang Feng. Llava-mini: Efficient image and video large multimodal models with one vision token. *arXiv preprint arXiv:2501.03895*, 2025b.
- Yi-Fan Zhang, Huanyu Zhang, Haochen Tian, Chaoyou Fu, Shuangqing Zhang, Junfei Wu, Feng Li, Kun Wang, Qingsong Wen, Zhang Zhang, et al. Mme-realworld: Could your multimodal llm challenge high-resolution real-world scenarios that are difficult for humans? *arXiv preprint arXiv:2408.13257*, 2024b.
- Baining Zhao, Jianjie Fang, Zichao Dai, Ziyou Wang, Jirong Zha, Weichen Zhang, Chen Gao, Yue Wang, Jinqiang Cui, Xinlei Chen, et al. Urbanvideo-bench: Benchmarking vision-language models on embodied intelligence with video data in urban spaces. In *Proceedings of the 63rd Annual Meeting of the Association for Computational Linguistics (Volume 1: Long Papers)*, pp. 32400–32423, 2025a.
- Baining Zhao, Ziyou Wang, Jianjie Fang, Chen Gao, Fanhang Man, Jinqiang Cui, Xin Wang, Xinlei Chen, Yong Li, and Wenwu Zhu. Embodied-r: Collaborative framework for activating embodied spatial reasoning in foundation models via reinforcement learning. In *Proceedings of the 33rd ACM International Conference on Multimedia*, pp. 11071–11080, 2025b.
- Hengguang Zhou, Xirui Li, Ruochen Wang, Minhao Cheng, Tianyi Zhou, and Cho-Jui Hsieh. R1-zero's "aha moment" in visual reasoning on a 2b non-sft model. *arXiv preprint arXiv:2503.05132*, 2025.
- Yiyang Zhou, Chenhang Cui, Jaehong Yoon, Linjun Zhang, Zhun Deng, Chelsea Finn, Mohit Bansal, and Huaxiu Yao. Analyzing and mitigating object hallucination in large vision-language models. In *ICLR*, 2024.
- Jinguo Zhu, Weiyun Wang, Zhe Chen, Zhaoyang Liu, Shenglong Ye, Lixin Gu, Yuchen Duan, Hao Tian, Weijie Su, Jie Shao, et al. Internvl3: Exploring advanced training and test-time recipes for open-source multimodal models. *arXiv preprint arXiv:2504.10479*, 2025.
- Chengke Zou, Xingang Guo, Rui Yang, Junyu Zhang, Bin Hu, and Huan Zhang. Dynamath: A dynamic visual benchmark for evaluating mathematical reasoning robustness of vision language models. *arXiv preprint arXiv:2411.00836*, 2024.

A PROMPT

A.1 SYSTEM PROMPT

```
SYSTEM_PROMPT

You are a helpful assistant.

# Tools
You may call one or more functions to assist with the user query.
You are provided with function signatures within <tools></tools> XML
↪ tags:
<tools>
{
  "type": "function",
  "function": {
    "name": "image_zoom_in_tool",
    "description": "Zoom in on a specific region of an image by
↪ cropping it based on a bounding box (bbox) and an optional
↪ object label.",
    "parameters": {
      "type": "object",
      "properties": {
        "bbox_2d": {
          "type": "array",
          "items": {
            "type": "number"
```

```

    },
    "minItems": 4,
    "maxItems": 4,
    "description": "The bounding box of the region to zoom in,
    ↪ as [x1, y1, x2, y2], where (x1, y1) is the top-left
    ↪ corner and (x2, y2) is the bottom-right corner."
  },
  "label": {
    "type": "string",
    "description": "The name or label of the object in the
    ↪ specified bounding box (optional).\"
  }
},
"required": [
  "bbox_2d"
]
}
}
</tools>

# How to call a tool
Return a json object with function name and arguments within
↪ <tool_call></tool_call> XML tags:
<tool_call>
{"name": <function-name>, "arguments": <args-json-object>}
</tool_call>

**Example**:
<tool_call>
{"name": "image_zoom_in_tool", "arguments": {"bbox_2d": [10, 20,
↪ 100, 200], "label": "the apple on the desk"}}
</tool_call>

```

A.2 USER PROMPT

USER_PROMPT

```

Question: {}

Think first, call image_zoom_in_tool if needed, then answer.
↪ Format strictly as: <think>...</think>
↪ <tool_call>...</tool_call> (if tools needed)
↪ <answer>...</answer>

```

B TRAINING DATA

B.1 DATA DISTRIBUTION

As shown in Figure 6, our training corpus is constructed from three distinct sources, each contributing a unique focus:

- **Visual Search (47%, 22k samples)**: To support the model’s visual grounding and fine-grained perception capabilities, we leverage the V^* dataset (Wu & Xie, 2024), which is derived from COCO2017 (Lin et al., 2014). This collection emphasizes natural image understanding, where accurate responses require identifying subtle visual cues and object-level distinctions.
- **ArxivQA (30%, 14k samples)**: To diversify the visual input types, we incorporate the ArxivQA dataset (Li et al., 2024b), which features scientific plots, diagrams, and schematic charts. These samples introduce structured visual semantics beyond natural scenes, enabling the model to better interpret abstract and symbolic visual representations.

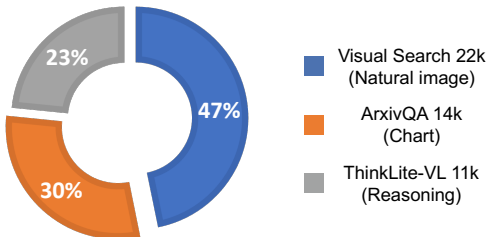


Figure 6: Distribution of Training Data.

- **ThinkLite-VL (23%, 11k samples)**: While the above datasets cover visual understanding and diagram comprehension, they are limited in reasoning variety. To address this, we include multimodal question answering examples from ThinkLite-VL (Wang et al., 2025b), focusing on tasks such as arithmetic reasoning, commonsense inference, and problem solving. This addition is intended to improve general reasoning robustness and mitigate modality-specific overfitting.

B.2 IMPACT OF TRAINING DATA

Table 10 reveals the critical role of training data composition. While unfiltered data (#1) offers minimal benefit, our curated, fine-grained data (#2) substantially boosts high-resolution image handling. However, this specialization induces catastrophic forgetting of reasoning skills. We address this by incorporating reasoning data (#3), which preserves mathematical abilities without sacrificing perception gains. To further enhance the model’s cognitive range, we introduce chart data (#4), which adds visual diversity and fosters complex relational reasoning. The results confirm a clear synergy: high-resolution data for perception, reasoning data for cognitive retention, and chart data for relational complexity. Consequently, our final dataset (#5) combines these complementary sources to comprehensively activate the model’s visual reasoning capabilities.

Table 10: **Impact of Training Data.** Fine represents the fine-grained data. HR denotes HR-Bench. Row #0 is the origin score of Qwen2.5-VL-7B.

#	Fine	Reason	Chart	High-Resolution			Basic VL Capability		Reasoning	
				V* Bench	HR-4K	HR-8K	ReasonSeg	POPE	MathVista	MathVerse
0				71.2	68.8	65.3	68.3	85.9	68.2	45.6
1	✓			86.9	68.9	67.3	69.0	86.6	67.0	42.9
2	✓			91.6	74.1	71.0	69.1	88.1	64.7	41.3
3	✓	✓		91.6	73.8	70.5	68.6	88.8	67.7	43.8
4	✓		✓	90.1	74.6	74.6	68.5	87.9	64.6	38.1
5	✓	✓	✓	90.1	75.1	72.6	68.6	87.7	70.1	47.3

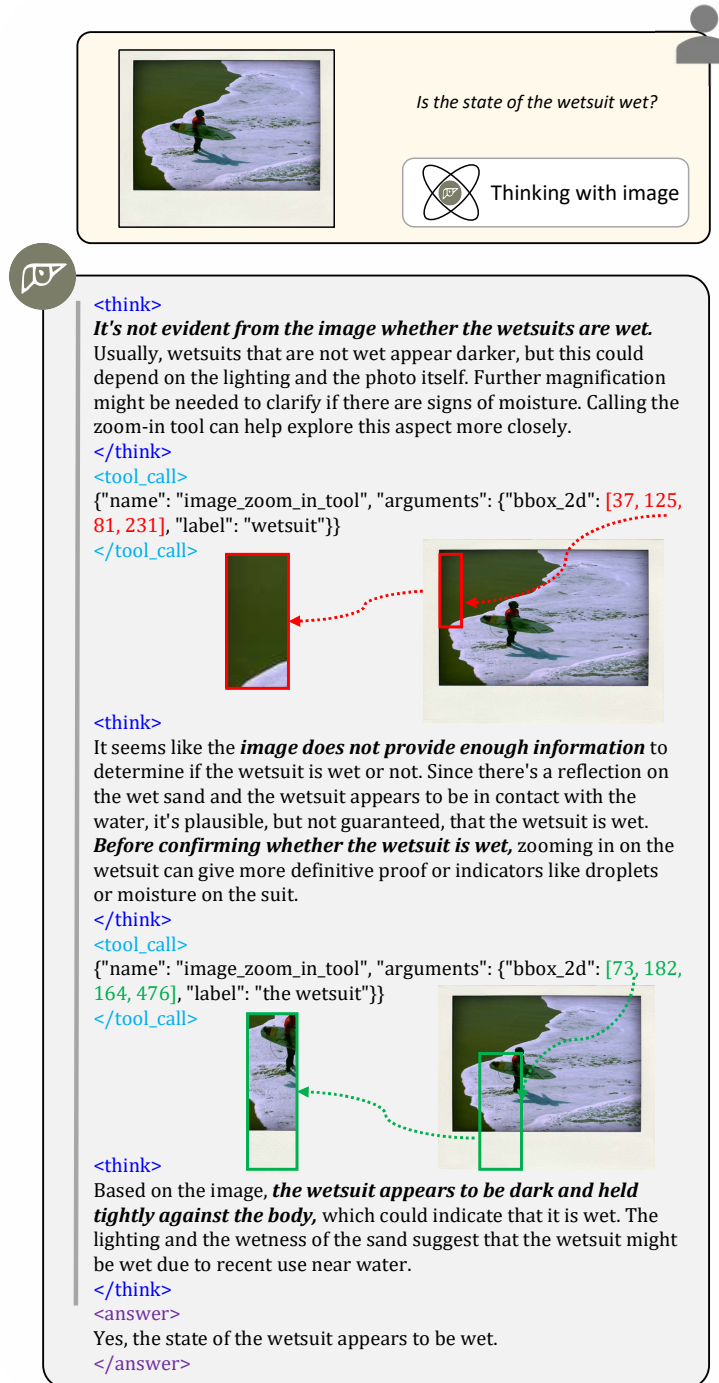
C CO-FIRST AUTHOR CONTRIBUTIONS

- **Chenxiao**: Conducted early-stage exploration, contributed the main coding, and conducted the experiments.
- **Jack**: Conducted early-stage exploration and performed evaluation.
- **Michael**: Contributed codebase, and conducted the experiments and analysis.
- **Ziwei**: Performed data curation, completed the main manuscript writing, and conducted analysis.

D MORE CASES

D.1 SUCCESSFUL CASES

- **Visual Search**





`<think>`
It's not evident from the image whether the wetsuits are wet.
 Usually, wetsuits that are not wet appear darker, but this could depend on the lighting and the photo itself. Further magnification might be needed to clarify if there are signs of moisture. Calling the zoom-in tool can help explore this aspect more closely.
`</think>`
`<tool_call>`

```

{"name": "image_zoom_in_tool", "arguments": {"bbox_2d": [37, 125, 81, 231], "label": "wetsuit"}}

```

`</tool_call>`





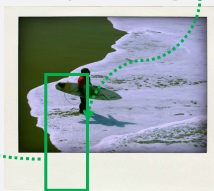

`<think>`
 It seems like the ***image does not provide enough information*** to determine if the wetsuit is wet or not. Since there's a reflection on the wet sand and the wetsuit appears to be in contact with the water, it's plausible, but not guaranteed, that the wetsuit is wet. ***Before confirming whether the wetsuit is wet***, zooming in on the wetsuit can give more definitive proof or indicators like droplets or moisture on the suit.
`</think>`
`<tool_call>`

```

{"name": "image_zoom_in_tool", "arguments": {"bbox_2d": [73, 182, 164, 476], "label": "the wetsuit"}}

```

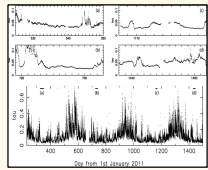
`</tool_call>`



`<think>`
 Based on the image, ***the wetsuit appears to be dark and held tightly against the body***, which could indicate that it is wet. The lighting and the wetness of the sand suggest that the wetsuit might be wet due to recent use near water.
`</think>`
`<answer>`
 Yes, the state of the wetsuit appears to be wet.
`</answer>`

Figure 7: Thinking Pattern: Visual Search.



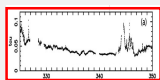
Based on the upper graphs, which labeled section (a-d) appears to show the least variability in the data?

 Thinking with image

<think>
 To determine which section shows the least variability, we need to examine the upper graphs (a, b, c, d). The variability can be assessed by how much the data fluctuates around the mean line. **Let's observe each section:**
</think>
<tool_call>

```
{"name": "image_zoom_in_tool", "arguments": {"bbox_2d": [124, 47, 955, 265], "label": "section (a)"}}
```

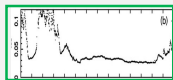

</tool_call>



<think>
 From the zoomed-in view of section (a), it's clear that the data fluctuates quite a bit, indicating higher variability. Let's proceed to examine the other sections:
</think>
<tool_call>

```
{"name": "image_zoom_in_tool", "arguments": {"bbox_2d": [79, 321, 986, 558], "label": "section (b)"}}
```

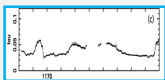

</tool_call>



<think>
 Section (b) shows less fluctuation compared to section (a), suggesting less variability. Now, let's zoom in on sections (c) and (d) to compare them more clearly.
</think>
<tool_call>

```
{"name": "image_zoom_in_tool", "arguments": {"bbox_2d": [1143, 30, 2003, 249], "label": "section (c)"}}
```

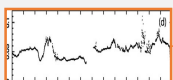

</tool_call>



<think>
 After zooming in on section (c), it appears that the data fluctuates less than in sections (a), (b), and (d), indicating the least variability. Let's **confirm** by examining section (d).
</think>
<tool_call>

```
{"name": "image_zoom_in_tool", "arguments": {"bbox_2d": [1090, 317, 2018, 558], "label": "section (d)"}}
```


</tool_call>



<answer>
 Section (c) appears to show the least variability in the data, so the answer is section (c).
</answer>

Figure 8: Thinking Pattern: Visual Comparison.



Is the window on the front of the vehicle *black and square*?

 Thinking with image



`<think>`

Looking at the image, the window on the front of the vehicle appears to be black and square. However, the resolution and angle of the photo may make it *difficult to see the details clearly*. If we need a closer look, we could use the zoom-in tool to get a better view of the window.

`</think>`

`<tool_call>`

```
{
  "name": "image_zoom_in_tool",
  "arguments": {
    "bbox_2d": [175, 44, 471, 137],
    "label": "window on the front of the vehicle"
  }
}
```

`</tool_call>`




`<think>`From the zoomed-in image of the vehicle's window, the window appears to be booking a possible diagonal from corner to corner, suggesting at least one dimension *might not be square*. However, considering the relation of the window to the vehicle's body, which seems to conform to an overall rectangular configuration, the window itself might be square, but confirmation would *require a closer view or a more specific tool analysis*.

`</think>`

`<tool_call>`

```
{
  "name": "image_zoom_in_tool",
  "arguments": {
    "bbox_2d": [222, 51, 455, 134],
    "label": "the window"
  }
}
```

`</tool_call>`




`<think>`The front window on the vehicle *appears to be* black and square, judging by the visible parts and typical vehicle design.

`</think>`

`<tool_call>`

```
{
  "name": "image_zoom_in_tool",
  "arguments": {
    "bbox_2d": [178, 37, 342, 112],
    "label": "the window"
  }
}
```

`</tool_call>`




`<think>`

Upon examining the image more closely, it appears the window on the front of the vehicle is *indeed black and square*.

`</think>`

`<answer>`

Yes, the window on the front of the vehicle is black and square.

`</answer>`

Figure 9: Thinking Pattern: Visual Confirmation.



Is the blazer black?

 Thinking with image

<think> The blazer seen through the windows of the building appears to be black, as per the overall color tone of the image. It's worn by a person walking away from the viewer towards the right of the frame. The blazer is distinguishable from the orange shirt worn by another individual in the background. Considering the color contrast and the blurred features, **the blazer can be identified as black.**

</think>

<tool_call>
 {"name": "image_zoom_in_tool", "arguments": {"bbox_2d": [94, 197, 143, 351]}}
</tool_call>




<think> Upon closer inspection, it is clear that the blazer is not black. Instead, it seems to have **black pants** with the blazer, **suggesting the person is wearing a red blazer.** Based on the visible colors and lack of black elements, the blazer in the image is not black, especially because it contrasts starkly with the red top

</think>

<answer>
 No
</answer>

Figure 10: Thinking Pattern: Hallucination Mitigation.



Is the color of the awning green?

 Thinking with image



`<think>`

Yes, the awning on the wall in the backdrop of the image **appears to be green**. The distinct color is evident against the other elements such as the parked vehicles. Let's **verify this by zooming in on the area** that includes the awning.

`</think>`

`<tool_call>`

```
{"name": "image_zoom_in_tool", "arguments": {"bbox_2d": [146, 5, 313, 92], "label": "the awning"}}
```

`</tool_call>`




`<think>`

The awning in the image **appears to be green**. However, to confirm this with high precision, especially considering the lighting, size, and resolution of the image, it may be beneficial to **zoom in on that region and examine it more closely**.

`</think>`

`<tool_call>`

```
{"name": "image_zoom_in_tool", "arguments": {"bbox_2d": [136, 3, 311, 75], "label": "awnings"}}
```

`</tool_call>`




`<think>`

The awning is clearly visible in the image. The image resolution allows for a clear distinction of colors, and **the awning has a distinct cobalt blue hue**. No confirmation tools would be needed as the awning color is observable.

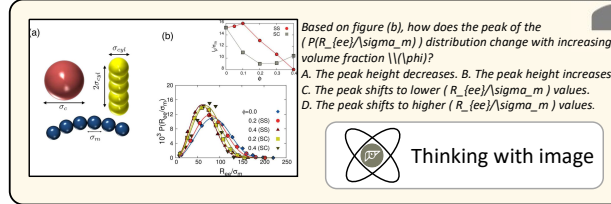
`</think>`

`<answer>`

Yes, the awning is blue. ❌

`</answer>`

Figure 11: Grounding Limitation.



<think>

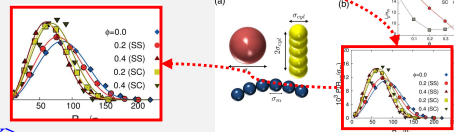
Observing figure (b), we need to focus on the position of the peaks of the distributions corresponding to different ϕ . As ϕ increases from 0.0 to 0.4, the peaks of the distribution shift to higher (R_{ee}/σ_m) values. This suggests that as the volume fraction ϕ increases, the most probable (R_{ee}) value also increases. Therefore, the correct answer is D.

</think>

<tool_call>

{"name": "image_zoom_in_tool", "arguments": {"bbox_2d": [1102, 707, 1520, 1057], "label": "peak position"}}

</tool_call>



<think>

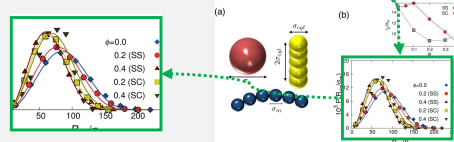
The zoomed-in view confirms that as the search space on the horizontal axis for (R_{ee}/σ_m) increases, the locations of the peaks **shift to the right**. This aligns with the observation in the full graph that the peaks move to higher values of (R_{ee}/σ_m) as ϕ increases. The peak position for higher values of ϕ (color-coded differently) shifts to higher (R_{ee}/σ_m) values compared to lower ϕ . Therefore, the correct answer is D.

</think>

<tool_call>

{"name": "image_zoom_in_tool", "arguments": {"bbox_2d": [1102, 707, 1520, 1057], "label": "peak position"}}

</tool_call>



<answer>

D. The peak shifts to higher (R_{ee}/σ_m) values. ✗

</answer>

Figure 12: Reasoning Limitation.

Figure 7: After an initial observation of the whole image, the model recognized that the current visual information alone was insufficient to determine whether it was wet, and acknowledged that factors such as lighting could cause misleading cues. It was therefore decided that a more detailed inspection was necessary. During the first tool invocation, grounding was inaccurate, and the cropped image failed to provide some clues. The model then conducted a second grounding step, this time actively focusing on the area surrounding the wetsuit in an attempt to locate more direct indicators—such as water droplets or visible signs of wetness. It also incorporated contextual cues from the surrounding environment, such as reflections on wet sand and the wetsuit’s contact with water. Ultimately, by combining zoomed-in visual details—such as the wetsuit’s dark coloration and how it clung to the body—with indirect environmental evidence, the model concluded that the wetsuit appeared to be wet.

- **Visual Comparison**

Figure 8: To determine which section exhibits the least data variability, the model sequentially zoomed in on the charts of four sections (a, b, c, and d), focusing on fluctuations around the moving average. Through comparison, it found that section (a) showed significant volatility, while section (b) was relatively less volatile. However, section (c) displayed the most stable pattern, with fluctuations clearly smaller than those in the other regions. Based on this analysis, the model concluded that section (c) has the least data variability.

- **Visual Confirmation**

Figure 9: In this case, the model was initially uncertain about the shape of the window. Through multiple invocations of the zoom-in tool and careful analysis of potential visual details, it gradually resolved its internal uncertainty and ultimately provided a confident answer.

- **Hallucination Mitigation** Figure 10: The model initially confused the colors of the pants and the blazer. However, by leveraging its perceptual capabilities and invoking the zoom-in tool to examine the enlarged region, it ultimately corrected the hallucination.

D.2 FAILED CASES

- **Grounding Limitation**

Figure 11: The model initially hypothesized that the awning was green. It then invoked the zoom-in tool for a closer inspection, maintaining its assumption while noting the need for more precise verification. However, during the second zoom-in, grounding drift occurred—the awning was no longer within the selected region, and instead, a blue area appeared. This misalignment led to a reversal in the model’s judgment, ultimately resulting in an incorrect answer.

- **Reasoning Limitation**

Figure 12: Although the model was able to accurately locate the position of figure (b) and invoke the tool for detailed inspection, it still lacked fine-grained understanding and reasoning capabilities. It failed to thoroughly analyze the trend changes in the zoomed-in curves, ultimately leading to an incorrect answer.

E LIMITATIONS

Although the simple end-to-end RL can elicit visual reasoning abilities, there still exist shortcuts, such as insufficient richness in the reasoning process and inaccurate target localization. We think these issues stem from limitations in the foundation model’s poor capabilities. We only utilized Qwen2.5-VL-7b, which has relatively weak fundamental capabilities due to its small model size.

F BROADER IMPACTS

Our exploration of interleaved multimodal chain-of-thought reasoning provides valuable insights for the future development of the AI community. By investigating how models can engage in step-by-step visual reasoning through interactive dialogues, we advance understanding of more transparent and interpretable AI systems. This research direction may inspire new architectures and training methodologies that better align with human reasoning processes.

G FUTURE WORK

Currently, our visual reasoning process only includes the crop operation. However, in real-world scenarios, a wider range of tools is needed, such as search and drawing auxiliary lines. We will explore the integration of additional tool utilization in our future work.